



A study on friction and wear characteristics of Fe–Cu–Sn alloy with MoS₂ as solid lubricant under dry conditions

S MUSHTAQ^{1,*}, M F WANI¹, M NADEEM³, K A NAJAR² and M MURSALEEN²

¹Tribology Laboratory, Mechanical Engineering Department, NIT Srinagar, Hazratbal, Srinagar 190006, India

²Mechanical Engineering Department, NIT Srinagar, Hazratbal, Srinagar 190006, India

³Metallurgical and Materials Engineering Department, NIT Srinagar, Hazratbal, Srinagar 190006, India

e-mail: shuhaibmushtaq@gmail.com; mfwani@nitsri.net; nadeem.nit.06@gmail.com;

najar.kaleem@gmail.com; mursaleen@nitsri.net

MS received 2 May 2019; revised 22 June 2019; accepted 21 August 2019; published online 22 November 2019

Abstract. Iron-based alloys are materials of choice for engineering applications such as bearings and gears owing to their low cost, ease of manufacture, high strength, availability, and good wear resistance and low coefficient of friction. In this study, Fe–Cu–Sn composite containing varying percentage of molybdenum disulfide (MoS₂) is developed using simple single stage compaction and sintering. The friction and wear behaviors of these composites were studied ball-on-disc tribometer in which EN8 steel ball was used. It was found that with the increase in percentage of MoS₂ from 0 to 3 wt% the coefficient of friction and wear rate substantially decreases from around 0.85 to 0.25. The wear mechanism in base composition (0% MoS₂) is observed to be adhesive and abrasive, whereas mild abrasive wear was observed in the 3 wt% MoS₂ composite. The hardness of composite was also found to improve with the increase in MoS₂ weight fraction.

Keywords. Fe–Cu–Sn alloys; MoS₂; coefficient of friction; wear; dry lubrication; bearing materials.

1. Introduction

Cost effectiveness is need of the hour in every industry and particularly in bearing and gears industries, and iron is one cheapest metals in addition to its excellent mechanical properties. Bearing materials can be produced economically by using Powder metallurgy (PM) techniques. PM produced parts are near-net shape which offers low cost production, and results in tight dimensional tolerances. In recent years, iron-based sintered tribomaterials have been considered over copper-based tribomaterials due to their lower cost and easy availability of iron powders [1]. Since a decade, high performance sintered iron-based self-lubricating composites have been developed [2] as a solution for combining a low friction coefficient with improved mechanical and wear resistance. Sintered composites contain high porosity, which reduce the mechanical strength and load-bearing capacity as compared to dense materials [3], however, according to Lim *et al* [4] porous materials have an ability to retain lubricants and release during use. In addition, wear debris produced during sliding interfaces may also be retained by pores and avoid further aggravation of wear and subsequently improves the tribosystem [5].

The tribological characteristics of sintered iron-based materials have been investigated by many researchers like

Sudhakar *et al* [6] and Liu *et al* [7]. It has been observed that the friction and wear resistance is substantially affected by the composition of material, percentage porosity, surface treatments and lubrication. It was also found by Khorsand *et al* [8] that the dense materials wear less. Under untreated conditions, the coefficient of friction ranges from 0.7 to 0.9 [9]. Sometimes additives are also used in iron-based sintered alloys in order to improve the friction and wear resistance [10] such as the addition of WS₂ nanoparticles to bronze graphite nanocomposite lead to low coefficient of friction [11]. The addition of graphite also improves the wear resistance in iron-based materials. Copper being a pearlite promoter is also added to improve the strength of iron and ultimately the strength of sintered composite [12]. The most used solid lubricants nowadays are MoS₂ and graphite worldwide [13, 14]. The mineral Molybdenite, having a metallic shine and dark blue coloration, occurs naturally as a compound in the earth crust [15]. It can be found commercially in the form of powder, suspensions, mixed in greases, as films or in composites with different matrices after proper processing and refining. The lubricant effect is based on its lamellar crystalline structure, where the Sulphur lamellae are bonded only by weak interaction (van der waals), which eases the shear [14]. The crystalline layers of MoS₂ will easily slide and orient parallel to the direction of relative movement in the occurrence of sliding, which provides the lubricating effect. The strong ionic bond

*For correspondence

between S and Mo provides the lamellae a high resistance to asperities penetration [16].

The objective of this paper is to investigate the coefficient of friction and wear rate at varying sliding distance and loads of the Fe–Cu–Sn alloys containing molybdenum disulfide as an additive. In addition to above objectives, bulk density and hardness of sintered composites have been evaluated.

2. Materials and methods

2.1 Material preparation

Iron, copper, tin and molybdenum di sulfide (MoS₂) powders were used to prepare four different compositions by single stage compaction and followed by sintering. The source and particle size characterisation of the above mentioned powders are given in table 1. The weighing of the powders was carried out in an electronic balance having an accuracy of ±0.0001 g and requisite proportions as given in table 2 were subsequently wet-mixed for 3 h using high-speed planetary ball mill (PULVERISITE 5, Classical line) at 150 rpm. After the completion of mixing, the mixed powders were dried and compacted at a pressure of 500 MPa and a green compacts of discs shapes with dimensions Ø30 × 8 mm were obtained. The green compacts/discs were then subjected to sintering at 1100 °C soaked 30 min in tabular furnace having 90% nitrogen and 10% hydrogen atmosphere. After the completion of sintering cycle the samples were furnace cooled by switching off the power.

2.2 Experimental method

The friction and wear tests were carried out on ball-on-disc universal tribometer by (Rtec Instruments, USA). The balls were made of EN-8 steel with a size of Ø9.5 mm and having Vickers hardness of 4.31 GPa. The discs were made of Fe–Cu–Sn composites with varying wt% of MoS₂ hereby referred as G0, G1, G2, and G3. The lower disc specimen rotates, whereas the upper ball specimen is fixed. Wear scar of Ø10 mm was made on the disc as the ball slides on it. The disc surfaces were first polished before subjecting to wear test by using 800, 1000, 1200 and 2000 grit size SiC emery papers on automatic polishing machine (Chennai

Table 2. Composition (wt%) selected for the study.

Composition no.	Fe	Cu	Sn	MoS ₂
G0	Bal	5	3	0
G1	Bal	5	3	1
G2	Bal	5	3	2
G3	Bal	5	3	3

METCO, India). The discs were then ultrasonically cleaned with acetone and subsequently dried in oven. The average surface roughness Ra for the discs was in the range of 0.13–0.25 µm, which was checked by a 3D surface profilometer (Rtec Instruments, USA). After the wear tests were completed, the data obtained from tribometer were used to calculate the coefficient of friction (COF).

The wear tests were carried out at varying sliding distance ranging from 250 to 1000 m, in a normal load range of 5–12 N, and at a sliding velocity of 0.025 m/s for all compositions. The weight loss was calculated the initial and final weight of samples. The wear volume was obtained from equation (1) as:

$$W_v = \frac{m}{\rho} \quad (1)$$

where W_v is the wear volume (mm³), m is the weight loss (g) and ρ is the density of the material (g/mm³). The wear coefficient (K_w) was obtained from equation (2) as:

$$K_w = \frac{W_v}{F_n S_d N x m} \quad (2)$$

where F_n is the applied load (N) and S_d is the sliding distance (m).

2.3 Characterization

The surface morphology of samples after wear test was examined under Optical microscope (Leica DM6000M), whereas the wear mechanisms were investigated by using scanning electron microscopy SEM (Hitachi S3600N) with an inbuilt energy dispersive spectroscopy (EDS). The bulk density and % porosity of samples were measured as per ASTM 2002 standards. Further details about the procedure is published elsewhere [13]. The densities and % porosity

Table 1. Source and characterization of the elemental powders.

Powder	Source	Particle size
Iron (Fe)	Sigma Aldrich, USA	80 µm; 99% purity
Copper (Cu)	SRL Laboratories, India	25–30 µm; 98% purity
Tin (Sn)	SRL Laboratories, India	10–25 µm; 98% purity
Molybdenum di sulfide (MoS ₂)	Sigma Aldrich, USA	30 µm; 99% purity

Table 3. Density and interconnected porosity of test materials.

	G0	G1	G2	G3
Bulk density (g/cm ³)	6.36	6.42	6.51	6.57
Interconnected porosity (%)	12.5	10.6	9.1	8.2

values of respective samples are given in table 3. The Vickers hardness of samples was found at loads ranging between 0.05 and 0.3 kgf with dwell time of 10 and 15 s. Indentations were made at five different locations for each load and dwell time.

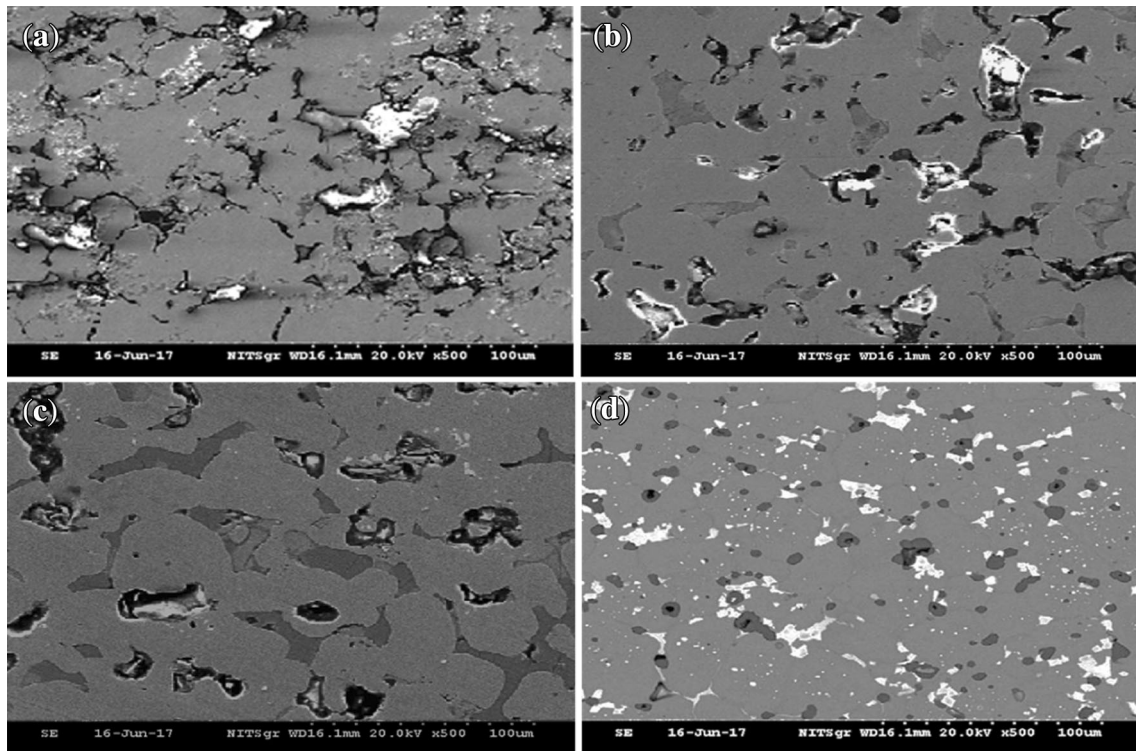


Figure 1. Micrographs of the sintered samples (a) G0, (b) G1, (c) G2 and (d) G3.

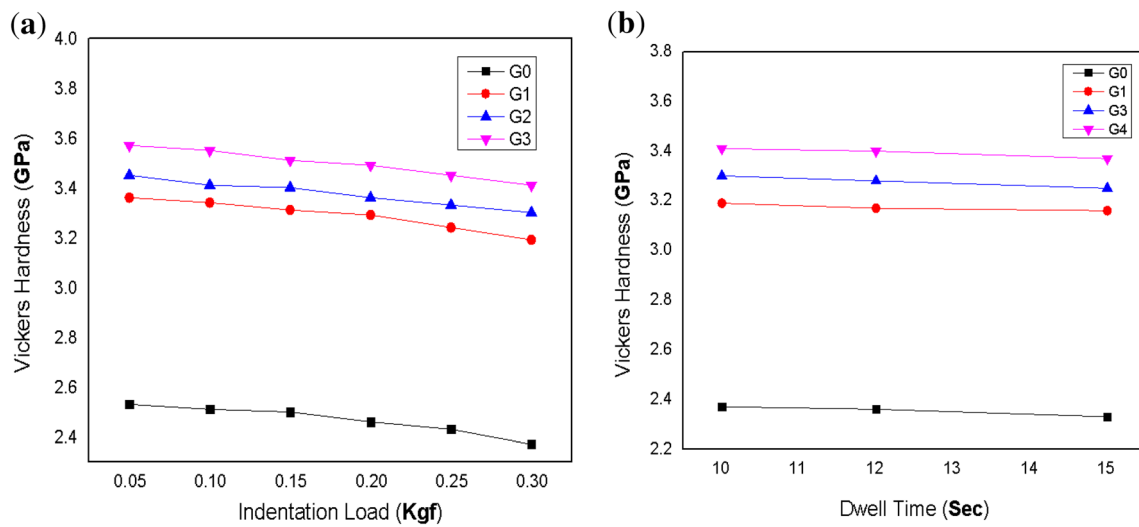


Figure 2. Average Vickers hardness versus (a) Indentation load and (b) Dwell time.

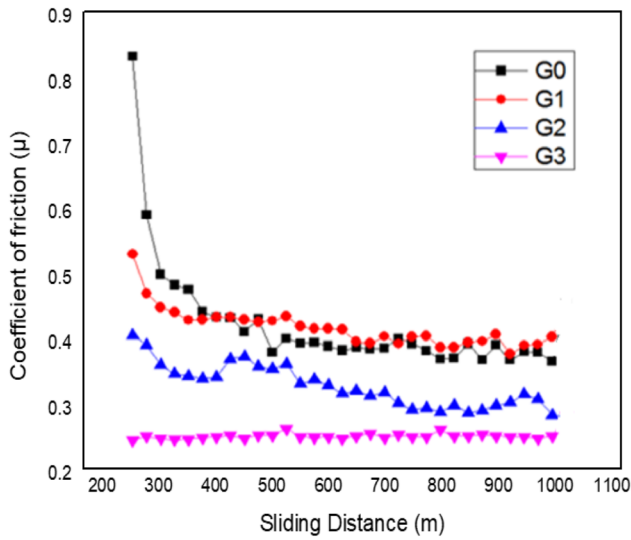


Figure 3. Coefficient of friction versus sliding distance.

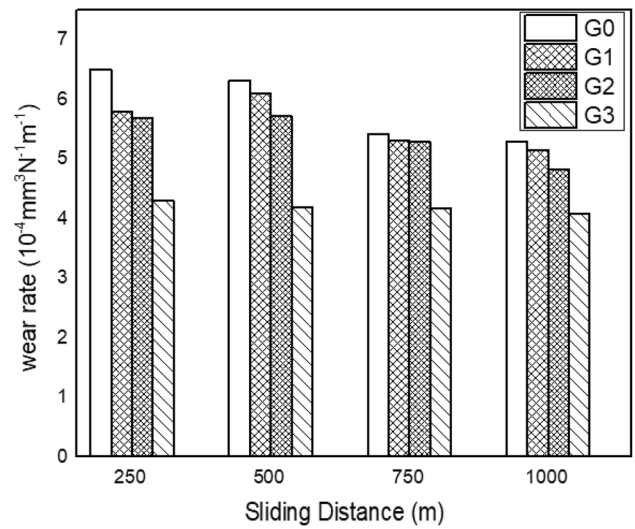


Figure 5. Wear rate versus sliding distance.

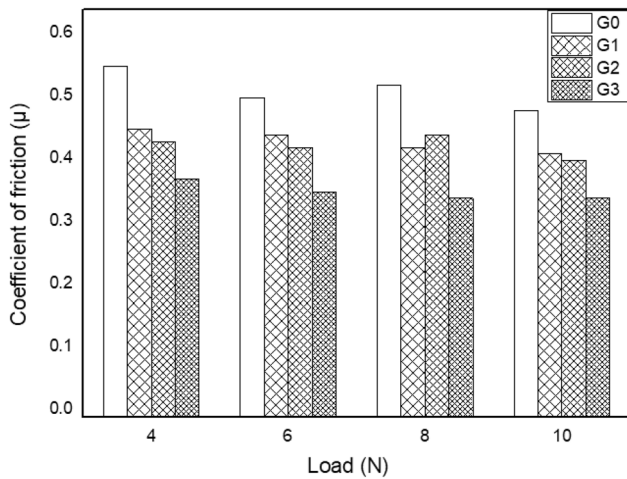


Figure 4. Coefficient of friction versus load.

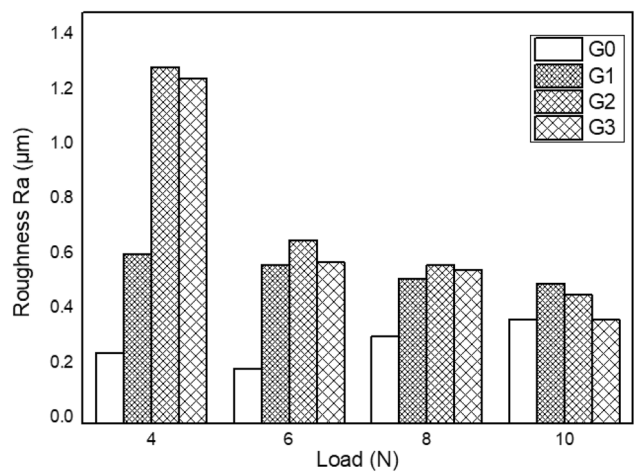


Figure 6. Surface roughness R_a versus load.

3. Results and discussion

3.1 Density and hardness

Interconnected porosity and density measurements carried out as per the standard on the sintered samples indicate that due to the addition of solid lubricant MoS_2 , an increase in density and decrease in the interconnected porosity were observed (table 3). This is also obvious from figures 1(a–d) showing the micrographs of the as-sintered samples G0, G1, G2 and G3. Large numbers of pores are observed in the base composition (G0), which correspond to the as sintered density of 6.36 g/cm^3 as compared with the composition (G3) which has higher wt% of MoS_2 shows higher density value of 6.57 g/cm^3 . Small and even distributions of pores

are observed in compositions containing MoS_2 as compared with base compositions (figures 1c, d). Density increases due to the increase in compressibility with the addition of solid lubricant. Densification in vacuum sintered stainless steel compositions was also found to improve with the addition of MoS_2 [17].

The average of Vickers microhardness values measured in the as-sintered samples are shown in figures 2(a, b). The hardness of 3 wt% MoS_2 (G3 composition) added material is very high compared with the base composition (G0). The higher density value and the presence of hard phase on the MoS_2 added compositions can be attributed to the increase in the hardness. A large amount of interconnected pores were present in the base composition, which yields a low hardness and strength compared with the materials with high density.

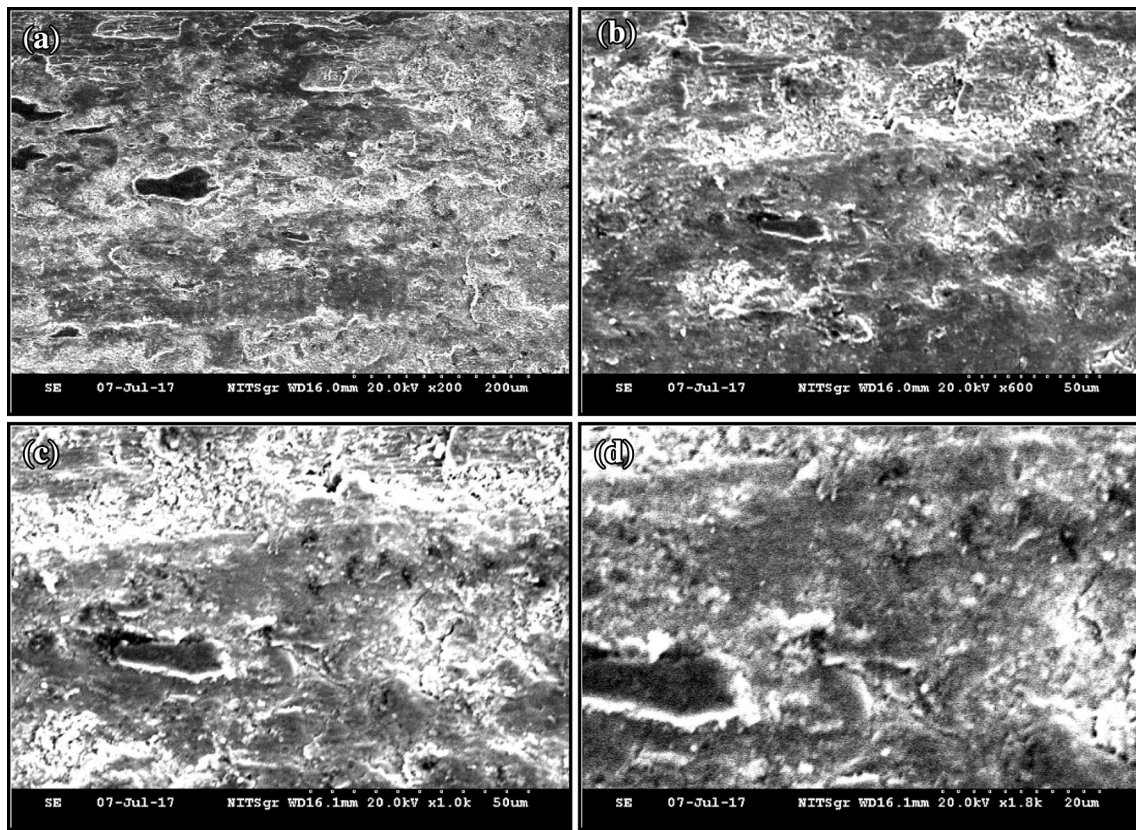


Figure 7. Wear micrographs of worn surfaces (a) G0, (b) G1, (c) G2 and (d) G3 compositions at applied normal load of 10 N.

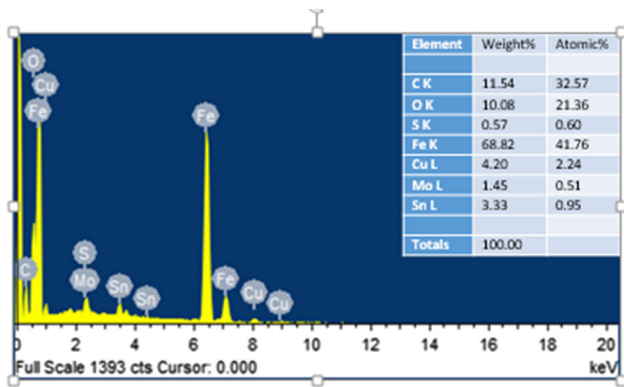


Figure 8. EDS showing the elemental composition of G3 sample.

3.2 Coefficient of friction (COF)

Figure 3 shows the variation of COF with sliding distance measured during dry sliding tests conducted at the applied normal load of 10 N. The initial COF at the beginning of the tests is higher for G0, G1, and G2 compositions and varied from 0.87, 0.56, and 0.43 for G0, G1, and G3 compositions, respectively. The initial higher values of COF is attributed to the direct metal to metal contact, due to which the friction traction increases at the asperity levels

and hence increase in COF observed. With further increase in sliding distance the COF decreases due to the solid lubricant MoS₂ forms the rich lubricant film between the sliding ball and disc due to which the COF values decreases and reaches steady state level. The values were observed as 0.52, 0.46, 0.35 and 0.28 for G0, G1, G2 and G3 compositions. Materials with 3 wt% of MoS₂ shows the least values of COF as compared with base composition without solid lubricant.

Figure 4 shows the steady state COF of the test materials at different normal loads investigated. At all applied normal loads the composition G3 exhibited the lowest COF and base composition G0 had the highest COF. The higher wt% of MoS₂ solid lubricant in G3 composition contributes to the decrease in COF.

3.3 Wear behavior

Wear rate based on the weight measurements carried out before and after the test of the Fe–Cu–Sn–MoS₂ composites (disc sample) is shown in figure 5. G3 composition with 3 wt% MoS₂ shows the lower wear rate than that of G0 composition without MoS₂ at all sliding distances. High COF and loose wear particles in the base composition lead to higher wear rate.

The surface roughness before and after the experimentation in all the samples were made to be same. The surface roughnesses of tested samples were measured by using 3D profilometer. Three to four samples of each composition were taken for measuring their surface roughness and the values are shown in figure 6. It can be clearly seen from figure 6 that the surface roughness value is $0.4 \mu\text{m}$ in the G0 composition at low applied load (4 N). The surface roughness increases at higher applied normal load (10 N) and the value is $0.52 \mu\text{m}$.

The low density of the G0 composition, the loose wear debris fill the pores leading to the smooth surface as shown in figure 6. In the base composition G0, the final surface roughness is about $0.23 \mu\text{m}$ at lower normal loads and increases with increasing load up to $0.36 \mu\text{m}$ at higher normal load (10 N) applied. In MoS_2 added compositions the surface roughness decreases with increase in normal load. In G3 composition the surface roughness of $1.21 \mu\text{m}$ were obtained at lower applied normal load (5 N) which is higher than G0 composition at lower applied normal load.

Figures 7(c, d) dark colored regions of smeared sulphides were observed on the wear tracks. The presence of solid lubricant leads to the formation of smoother surface in G1, G2 and G3 compositions as compared to G0 (without MoS_2) composition which contributes to the lower COF. The G3 composition with higher wt% of MoS_2 shows the lower COF than G2 and G1 composition. Addition of MoS_2 in the investigated materials increases the hardness of the material compared with G0 (without MoS_2) composition. The strength and hardness of the material is directly proportional to the wear resistance. G3 composition with maximum wt% of MoS_2 shows the higher hardness leads to high wear resistance. The loose wear particle lead to the formation of three-body abrasion in G0 composition and due to low strength the wear resistance reduces. Figure 8 shows the EDS analysis which gives the elemental composition of the presence of sulphides due to which the reduced coefficient of friction can be depicted.

4. Conclusion

- Fe–Cu–Sn alloy with MoS_2 as solid lubricant are developed by using PM technique for application in machine elements such as bearings and gears.
- Density, interconnected porosity and Micro-hardness (HV) increase with the addition of solid lubricant MoS_2 .
- G3 composition (with 3 wt% MoS_2) shows the reduced value of COF compared with the G0 composition (without MoS_2).
- G3 composition contributes to high wear resistance due to the increased density and hardness.
- MoS_2 added samples with low COF causes low wear rate compared with G0 composition.

Nomenclature

MoS_2	molybdenum di sulfide
PM	powder metallurgy
W_v	wear volume
K_w	wear coefficient
S_d	sliding distance
COF	coefficient of friction

References

- [1] Teisanu G and Gheorghe S 2011 Development of new PM iron-based materials for self-lubricating bearings. *Adv Tribol.* 248037
- [2] de Mello J D B, Binder C, Hammes G and Klein A N 2013 Effect of the metallic matrix on the sliding wear of plasma assisted debinded and sintered MIM self-lubricating steel. *Wear* 301: 648–655
- [3] De H I M, Mello J D B, Binder R and Klein A N 2001 Effect of compaction pressure and powder grade on microstructure and hardness of steam oxidised sintered iron, *Powder Metall.* 44(1): 53–61
- [4] Lim S C and Brunton J H (1986) The unlubricated wear of iron. *Wear* 113: 371–382
- [5] Ahn H S, Kim J Y and Lim D S (1997) Tribological behavior of plasma-sprayed zirconia. *Wear* 203: 77–87
- [6] Sudhakar K V, Sampathkumaran P and Dwarakadasa E S 2000 Dry sliding wear in high-density Fe–2%Ni based P/M alloys. *Wear* 7: 202–242
- [7] Zuomin L and Childs T H 2004 The study of wear characteristics of sintered high-speed steels containing CaF₂, MnS, TiC additives at elevated temperature. *Wear* 40: 257
- [8] Seraji H R, Khorsand H, Habibi S M, Yoozabashizadea H, Janghorban K and Reihani S M S 2002 The role of heat treatment on wear behavior of powder metallurgy low alloy steels. *Mater Des.* 23: 67–70
- [9] Candela N, Plaza R, Rosso M, Velasco F and Torralba J M 2001 Radial crushing strength and microstructure of molybdenum alloyed sintered steels. *J Met Process Technol.* 119: 7–13
- [10] Rapoport L, Feldman Y et al 1999 Inorganic fullerene-like material as additives to lubricants: structure-function relationship. *Wear* 972: 225–229
- [11] Velasco F, Gordo E, Isabel R, Ruiz Navas E M and Bautista A 2001 Mechanical and wear behavior of high-speed steels reinforced with TiCN particles. *Int J Refract Mater Hard Mater* 19: 319
- [12] Annamalai R, Upadhyaya A and Agrawal D 2013 An investigation on microwave sintering of Fe, Fe–Cu and Fe–Cu–C alloys. *Bull Mater Sci.* 36: 447–456
- [13] Shuhaib S and Wani M F 2017 Self-lubricating tribological characterization of lead-free Fe–Cu based plain bearing material. *J Tribol.* 12: 18–37
- [14] Miyoshi K 2001 *Solid lubrication fundamentals and applications.* Taylor & Francis, p. 9

- [15] Busch C, Dresel W and Mang T 2007 *Solid lubricants and lubrication*, 2nd ed. Wiley-Vch, pp. 231–235
- [16] Lansdown A 1999 *MoS₂ lubrication*. Cambridge: Elsevier, p. 7.4
- [17] Sustarsic B, Kosec L, Jenko M and Leskovsek 2001 Vacuum sintering of water-atomized HSS powders with MoS₂ additions. *Vacuum*. 61: 471–477